

---

# The Thermal Conditions and the Strength of a Spent Fuel Package: Analysis and Test

E.D. Fedorovitch

*Polzunov Scientific and Development Merger on Research and Designing the Power Equipment, Leningrad, Union of Soviet Socialist Republics*

## Abstract

The paper describes the results of investigation aimed at finding thermal and structural analysis methods applicable to transport and storage spent fuel packages.

The expressions for heat transfer analysis of horizontal and vertical fuel assemblies under natural convection are derived from test data of 15 electrically heated rod bundles.

The information is given on a computer code for analysis of a package fire-associated accident thermal condition and Subsequent cooling.

The advantages of design-basis proof of a package compliance with IAEA regulations have been discussed. The specific examples demonstrate that the developed thermal and structural analysis methods give the possibility to avoid full-scale package tests without reliability degradation.

Experimental investigation and expressions for thermal analysis of fuel assemblies under natural convection.

The expressions for heat transfer analysis of horizontal fuel assemblies under natural convection are derived from test data of 13 electrically heated rod bundles, installed in bundle wrappers of different forms.

The same expressions can be used for the analysis of heat transfer between fuel assemblies and a horizontal spent fuel package inner shell.

The following parameters have been changed during the

test:

- a form (hexahedral, round, rectangular) of a bundle wrapper,
- bundle arrangement;
- rod row number in a bundle of a hexagonal
- arrangement (7 -, 19, -, 37-, 331 - rod bundles),
- relative pitch ( $S/d = 1,165 + 2,31$ ),
- surface blackness degree of heat releasing rods and heat absorbing wrapper;
- heat release,
- gas coolant pressure ( $0,3 \text{ kPa} \leq P \leq 1,8 \text{ MPa}$  ).

In most tests heat from a wrapper rejected to cooling water, circulating in the space between the wrapper and an experimental model outer shell. Because of high rate of cooling water the temperatures all over the wrapper surface were closely spaced. In some tests heat from a wrapper rejected directly in ambient air by air natural convection and thermal radiation, that is the wrapper was not under isothermal condition.

Rods and wrapper temperatures over the middle (in length) bundle section have been measured by thermocouples.

The total surface area of multirod bundles  $F_{cm}$  was considerably greater than that of a wrapper  $F_k$ , and coolant temperature around the rod was close to rod temperature, that made possible to plot the isotherms of coolant over a bundle sections. Natural convection development have been investigated by the analysis of temperature distribution throughout the rods and the character of coolant isotherms in a model section. When space in 75-rod model is filled with air  $P = 0,1 \text{ MPa}$ , the isotherms have a form close to circles, that demonstrates poor natural convection (fig. 1a). As the air pressure goes up to  $P = 0,7 \text{ MPa}$ , the natural convection enhances and isotherm character changes (Fig. 1b).

In 331-rod bundle with section size greater than that of 75-rod one developed convection is observed even at air pressure  $P = 0,1 \text{ MPa}$  (Fig. 1 B), and at air pressure  $P = 0,7 \text{ MPa}$  isotherms in the main part of a bundle section becomes rather flat (Fig. 1 F).

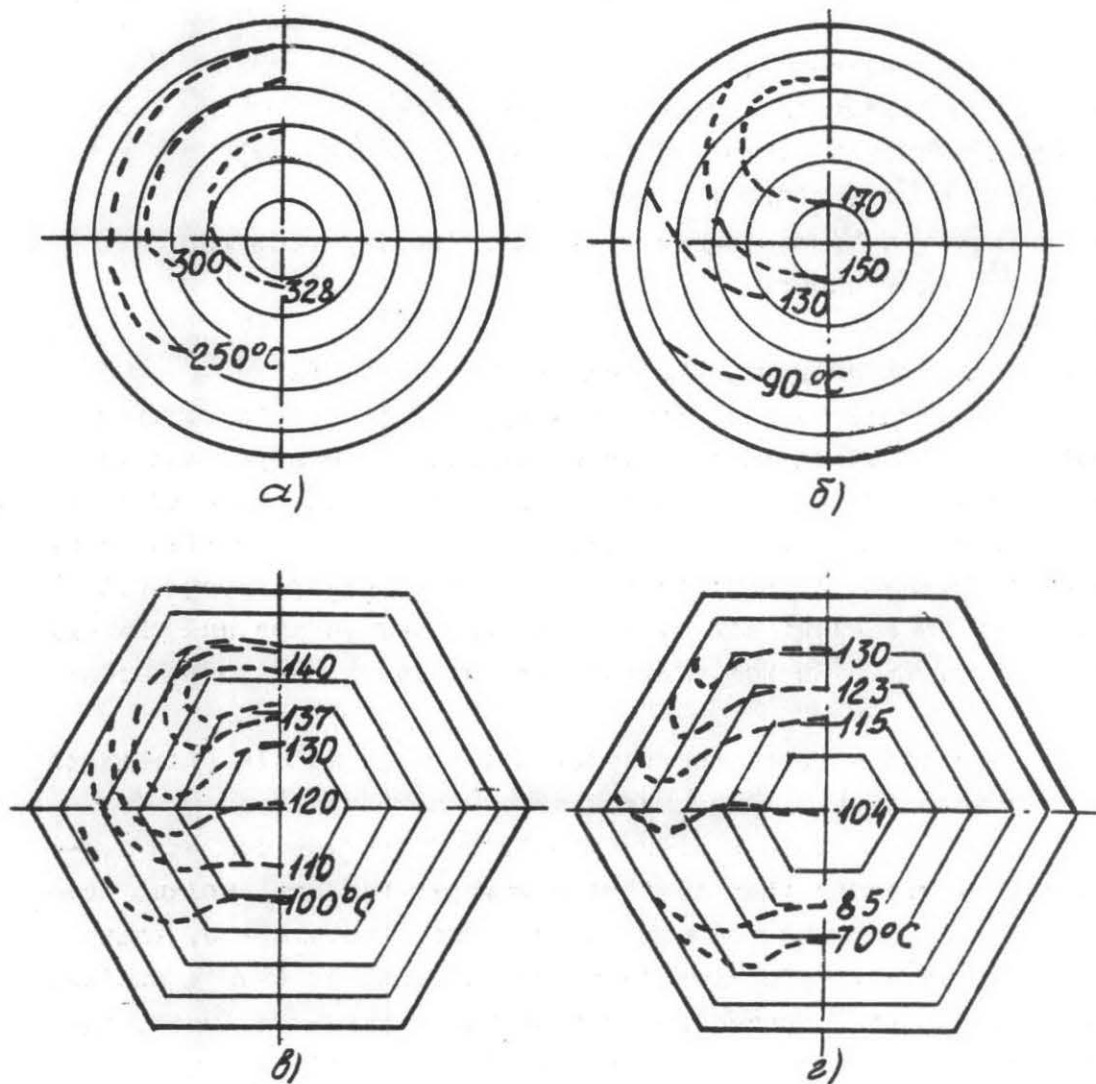


Fig.1. Isotherms in rod bundle section

- |                   |                   |
|-------------------|-------------------|
| a) $P = 0,1$ MPa; | $q_e = 12$ Wt/m;  |
| b) $P = 0,3$ MPa; | $q_e = 6$ Wt/m;   |
| c) $P = 0,1$ MPa; | $q_e = 1,8$ Wt/m; |
| d) $P = 0,7$ MPa; | $q_e = 4,7$ Wt/m; |

Natural convection development is investigated by the analysis of temperature patterns in a 37-rod bundle section ( $S/d = 1,165$ ) when the bundle space is filled with air or motor oil. At air pressure  $P = 0,1$  MPa or at a low heat release per a bundle rod ( $q_e = 3,6$  Wt/m) when the bundle space is filled with oil, the temperature pattern is close to axially symmetric one (Fig. 2a, 6). As the pressure  $P = 0,9$  MPa and the heat release ( $q_e = 31,6$  Wt/m) go up, the temperature along the bundle section height increases with the slight change of the rod temperatures in a horizontal row (Fig. 2b, 2). When the bundle space is filled with water pronounced natural convection is observed even at a low heat releases.

The character of the temperature patterns and the isotherm form show, that under developed natural convection the heat from rods transfers to coolant, then the heated coolant moves upwards, covering the largest part of the bundle section. The coolant motion downwards and cooling take place in a relatively narrow clearance between a wrapper and an outer rod row.

Natural convection enhancement raises the rate of heat transfer. For example, during the test of 37-rod bundle ( $S/d = 1,38$ ) the maximum temperature of a heated rod reduced from  $181^\circ\text{C}$  to  $81^\circ\text{C}$ , as air pressure increased from  $0,1$  to  $0,9$  MPa with heat release per rod  $q_e = 11$  Wt/m.

Test data showed that the increase of  $S/d$  caused the rod temperature reduction. The reduced hydraulic resistance in a natural circulation circuit seemed to account for this result.

As the package thermal analysis must take account of the temperature of the most heated fuel assembly  $t_{cm}^{\max}$  and the pressure in the package space, which depends on the average coolant temperature, affected by the average fuel assemblies temperature  $\bar{t}_{cm}$ , we obtained criterion functions for heat transfer coefficients calculation, permitting these temperatures to be determined. Two temperature drops have been studied ( $t_{cm}^{\max} - \bar{t}_k$ ) and ( $\bar{t}_{cm} - \bar{t}_k$ ), where  $\bar{t}_k$  - average wrapper surface temperature in the middle (in bundle length) section.



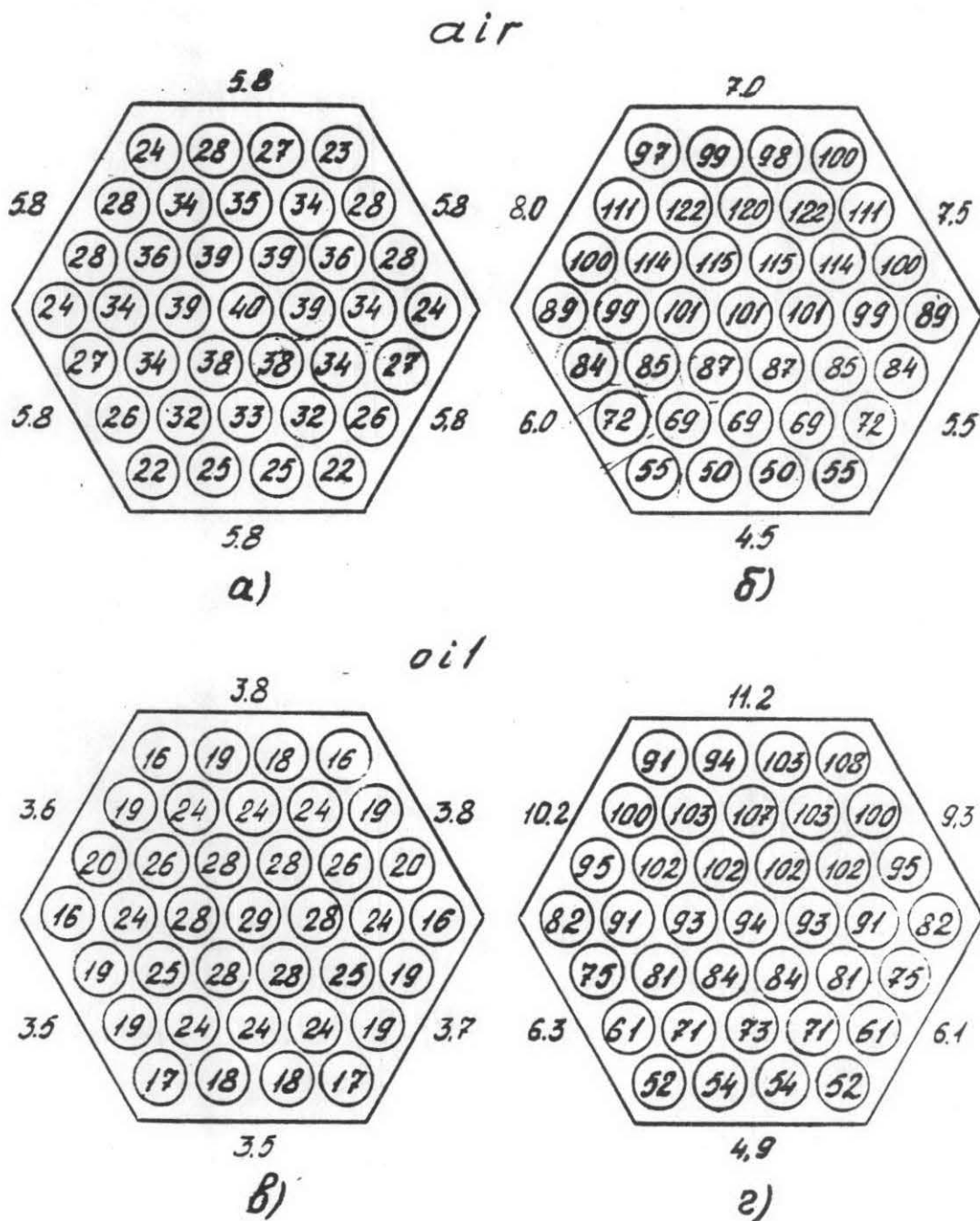


Fig.2. Temperature distribution over 37-rod bundle section  
( $S/d = 1.165$ )

a)  $P = 0,1$  MPa;

b)  $P = 0,9$  MPa;

c)  $q_e = 3,6$  Wt/m;

d)  $q_e = 31,6$  Wt/m;

In test data processing the heat transfer from coolant to a wrapper considered to be a basic process, and in coolant temperature calculation the allowance of equality of heat transfer coefficient from rods to coolant  $h_{cm-m}$  and from coolant to a bundle wrapper  $h_{m-k}$  had been made.

The design coolant temperatures  $t_m$  and  $t'_m$  were determined from the equations:

$$h_{cm-m}(\bar{t}_{cm-m} - t_m)F_{cm} = h_{m-k}(t_m - \bar{t}_k)F_k$$

and

$$h'_{cm-m}(t_{cm}^{max} - t'_m)F_{cm} = h'_{m-k}(t'_m - \bar{t}_k)F_k$$

The basic temperature drops and temperatures were calculated from the equations.

$$\begin{cases} \Delta t = t_m - \bar{t}_k \\ t_{onp} = 0.5(t_m + \bar{t}_k) \end{cases} \quad \begin{cases} \Delta t' = t'_m - \bar{t}_k \\ t'_{onp} = 0.5(t'_m + \bar{t}_k) \end{cases}$$

The data, obtained during the test of horizontal rod bundles, were presented in the form of equations:

$$Nu \left( \frac{T_m}{T_k} \right)^n = f(Ra \cdot \frac{s}{d}); \quad Nu' \left( \frac{T_m}{T_k} \right)^n = f'(Ra' \cdot \frac{s}{d}),$$

where

$$Nu = Q_{KOHb} \cdot l / (F_k \cdot \Delta t \cdot \kappa); \quad Nu' = Q_{KOHb} \cdot l / (F_k \cdot \Delta t' \cdot \kappa');$$

$$Ra = \frac{g\beta}{\nu\alpha} \cdot \Delta t \cdot l^3; \quad Ra' = \left( \frac{g\beta}{\nu\alpha} \right)' \cdot \Delta t' \cdot l^3$$

$Q_{KOHb}$ . - heat, transferred by convection from rods to a bundle wrapper;

$Q_{KOHb} = (Q - Q_{pag})$  - for gases

$Q_{KOHb} = Q$  - for liquids.

The bundle wrapper perimeter is used as a characteristic linear dimension.

To our opinion the ratio  $(T_m/\bar{T}_k)^n$  takes into account the fact that radiative heat transfer enhancement caused the temperature pattern change, worsening natural convection.

$$n = 0,5 \text{ (for gases) ; } n = 0 \text{ (for liquids)}$$

Data-averaged curve for 13 test rod bundles, used for average rod temperatures calculation is shown in Fig. 3. To carry out bundles thermal analysis the average heated surface temperature should be determined in the earlier stages of calculation, and the temperature  $\bar{T}_{cm}$  should be specified. The validity of the specified data is verified by the comparison of the calculated and specified values of heat flow  $Q$ . The radiative term of the heat flow  $Q$  pag could be defined by the empirical function, obtained by the authors /1/.

To determine the maximum rod temperatures  $t_{cm}^{max}$  the function is obtained similar to that shown in Fig. 3. The functions are meant for the horizontal rod bundle thermal analysis under developed natural convection, when the space between rods is filled by coolant with the Prandtl number  $Pr = 0,7 + 5000$ .

The boundary of the transition from the developed natural convection to heat transfer in the rod bundles by heat conduction and radiation (gas coolants) or only by heat conduction (liquid collants) have been determined.

The functions character indicated that the natural convection appreciably affects the multi-rod bundle thermal condition not only when a liquid coolant is used, but when the bundle space is filled with a gas, even the gas pressure is close to 0,1 MPa.

The functions are used for the horizontal packages thermal analysis, when the average and maximum fuel assemblies temperatures are determined from the specified heat release.

The same functions can be used for the calculation of the limiting residual fuel assembly heat release, if the limiting fuel assembly shell temperature is specified. The above thermal analysis methods are also valid in the cases when the assemblies are encased in leaktight canisters to improve their security. The obtained functions have been used for the

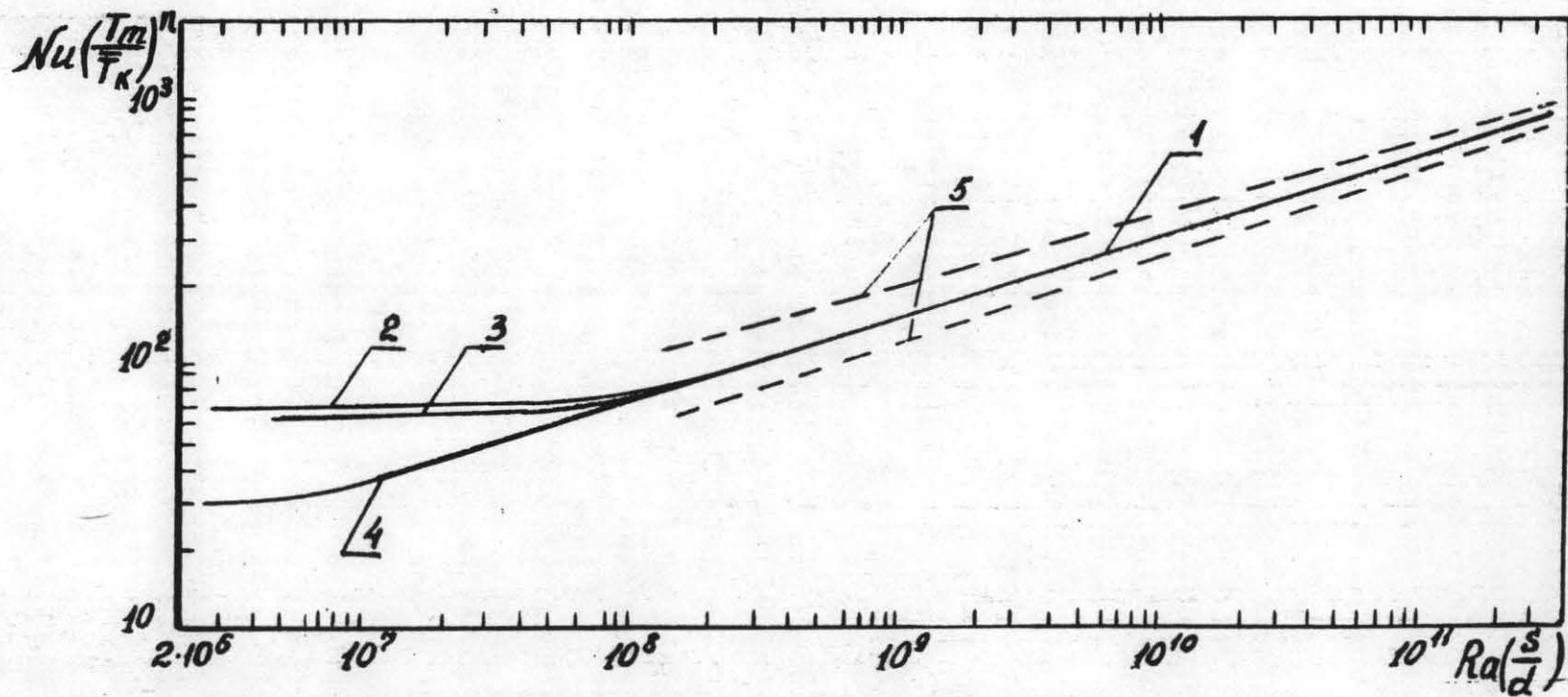


Fig.3. Function  $Nu \left( \frac{T_m}{T_k} \right)^n = f \left( Ra \frac{S}{d} \right)$  for horizontal rod bundles (t - averaged)  
 1 - average curve; 2 - 7 rods,  $S/d = 1,38$ ; 3 - 37-rods,  $S/d = 1,165$ ;  
 4 - 19 rods,  $S/d = 1,38$ ; 5 - boundary of test data spread



thermal analysis of the VVER-1000 spent fuel packages. The calculated values  $t_{om}^{max}$  and the results measured in the test of the package, filled with the air at barometric pressure, are in good agreement.

The heat exchange in vertical rod bundles, encased in leak-tight tubes (canisters), filled with a gas has been studied in two electrically heated models. A 37-rod bundle of hexagonal arrangement had a heated length  $L = 1,27$  m and was encased in a hexahedral shell (canister).

The model had a separable outer cylindrical shield with the water circulating in the space between the shell and the cylindrical shield. When heat was rejected to water, the shell surface was practically isothermal; when heat was removed directly into ambient air, the shell temperature increased and changed along the model height. The tests were carried out at air pressure in a canister case in the 0,3 kPa - 0,8 MPa range.

The second bundle consisted of 18 heated rods with  $d = 13,5$  mm ( $S/d = 1,185$ ) (the central tube was not heated). The centres of 6 inner row tubes were situated in the vertices of a hexahedron, and the centres of 12 outer tubes were equally spaced on a circle 620 mm in diameter. The bundle heated length was 2,845 m. The bundle was placed in a cylindrical canister the minimum distance between outer tube surface and the canister case was 11 mm. The minimum gap between tube rows was 2,5 mm. The heat from the canister case was rejected into a cooling water. The tests were carried out at air pressure in the canister space in the 0,3 kPa + 1,6 MPa range.

The Fig. 4 shows the temperature distribution along the 37-rod bundle height and rows at  $P = 0,1$  and 0,8 MPa. At  $P = 0,1$  MPa (Fig. 4a) the temperature of a corner and straight rods is constant along the main part of the bundle height that came as the evidence of the absence of the coolant circulation in the canister space. The heat transfer between rods and from the outer row to the canister case occurs by radiation and heat conduction. The air pressure increase gives the rise of the rods temperature along the whole

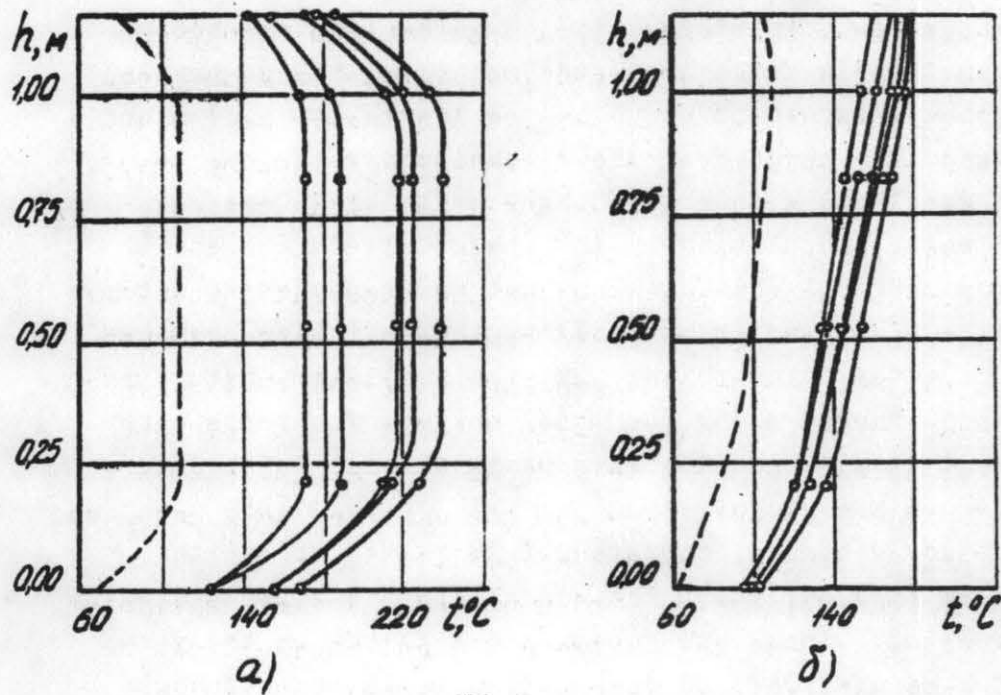


Fig.4. Temperature distribution throughout vertical 37-rod bundle.

a)  $P = 0,1$  MPa;

b)  $P = 0,8$  MPa

bundle height and the decrease of the radial temperature drop between the rods. It points to the emergence of natural convection contour with the coolant heating in the motion upwards in rod gaps and the coolant cooling in the motion downwards along the canister case (Fig. 48).

Fig. 5 shows the temperature distribution throughout the 19-rod bundle. The temperature elevation have not been recorded throughout the main part of the bundle height up to pressure  $P = 0,4$  MPa (Fig. 5a and 5b). The following pressure elevation gives the temperature rise along the rod height (Fig. 5c).

The 19-rod bundle test data at the constant temperature along the bundle height revealed the thermal-hydraulic conditions, which were not observed in the 37-rod bundle. So at the pressure elevation from 0,1 to 0,4 MPa the temperature drop between rod rows have been unchanged, and the temperature drop between the outer row and the canister case have been substantially decreased (Fig. 5a, 5b).

As the gap between the rod rows and the case is significantly larger, than that between the rod rows, it can be anticipated that small-scale vortexes emerge in the large gap and raise the rate of heat transfer.

Three typical conditions have been revealed in vertical rod bundles, encased in leak-tight canisters:

- natural convection is absent and conductive and radiative heat transfer takes place in radial direction (radiation - conduction condition)
- natural convection causes the emergence of small-scale vortexes, raising the rate of heat transfer (radiation - conduction condition with small-scale vortexes)
- the closed contour of natural convection develops in the canister, spreading all over the bundle height. The main part of the rod heat transfers to the canister case by the contour (radiation - convection conduction with developed convection).

For radiation - conduction condition the analytical techniques have been developed allowing the average rod temperature to be calculated consistently, beginning from the outer row.

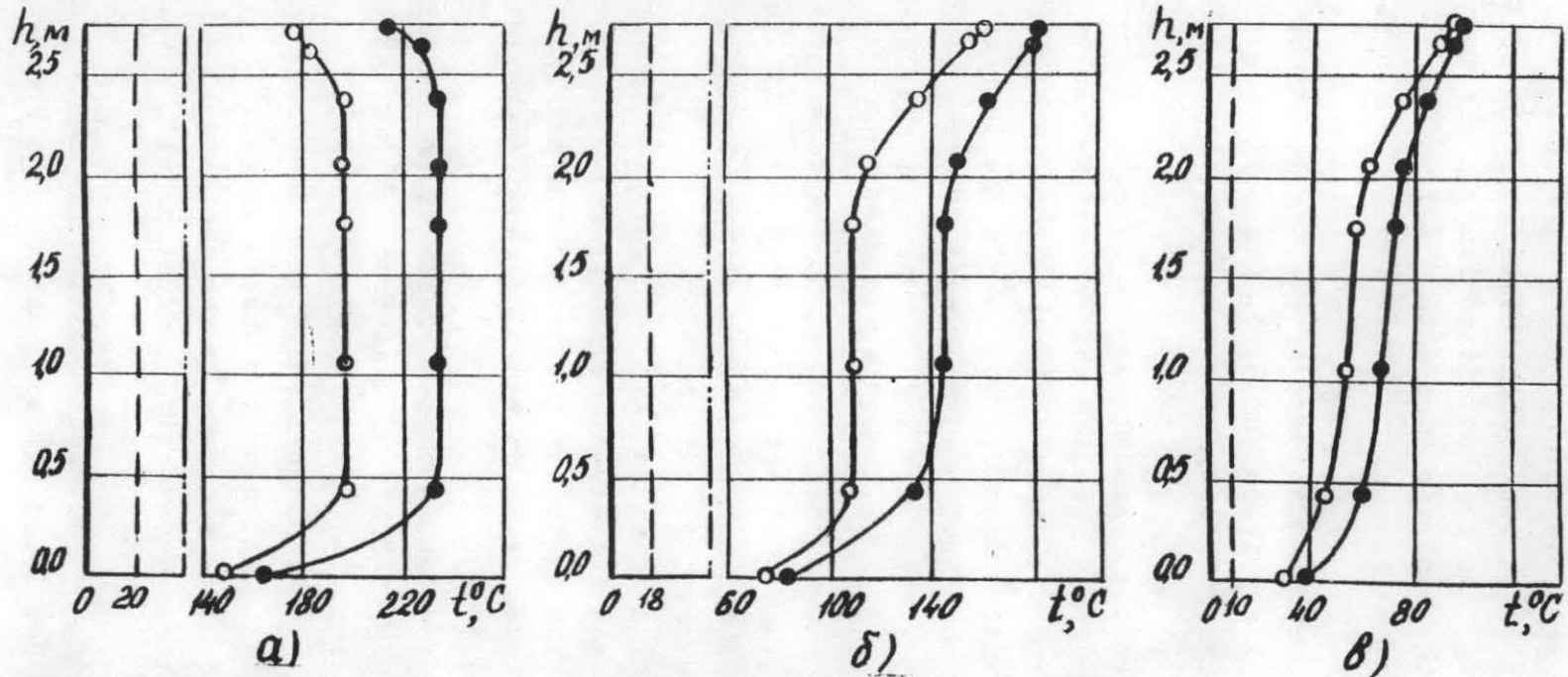


Fig.5. Temperature distribution throughout vertical 19-rod bundle.

a)  $P = 0,1$  MPa;

$P = 0,4$  MPa;

$P = 1,3$  MPa.

● - an inner row; ○ - an outer row;

--- - shell temperature



The salient points of techniques and the assumptions made are presented in the paper /2/.

The vertical rod bundles thermal analysis in the presence of small-scale vortexes, raising the rate of radial heat transfer can be made with help of the equations for conductive heat transfer calculation and an equivalent heat conduction coefficient  $K_{ЭК} = E_K \cdot K$ .

The equations take the form:

$$Q^{КОНБ} = E_K \cdot K' \cdot \Delta t' \cdot X ; \quad Q^{КОНГ} = \kappa'' \cdot \Delta t'' \cdot X$$

where:  $Q^{КОНБ}$ . - convective heat flow in the gap between rods or in the gap between the outer rod and the canister case;

$Q^{КОНД}$ . - conductive heat flow

$E_K$  - convection coefficient

$K$  - gas heat conduction coefficient at an average temperature in a gap (t);

$\Delta t$  - an average temperature drop between heat exchanging surfaces

$X$  - factor to account for geometry effect on conductive heat transfer between rod rows or the outer row and the case.

Ignoring the geometry factor  $X$ , the experimental values of  $E_K$  could be calculated with help of the temperature drops, obtained for the conditions, when the temperature along the main part of the rods height was unchanged (Fig. 5 б) and for vacuum conditions, when there was not natural convection and gas remained a continuous medium.

$$E_K = Q^{КОНБ} \cdot \kappa'' \cdot \Delta t'' / (Q^{КОНГ} \cdot K' \cdot \Delta t')$$

The curve in Fig. 6 allows the convection coefficient  $E_K$  to be calculated and determines the boundary between radiative - conductive conditions and these with small-scale vortexes.

In the number Ra calculation the minimum gap between rod rows or between the outer row and the canister case is a characteristic linear dimension.

The ratio  $Q^{КОНБ} / Q^{КОНД}$ . in the equation above is not a convection coefficient, as the values  $Q^{КОНБ}$ . and  $Q^{КОНД}$ . have

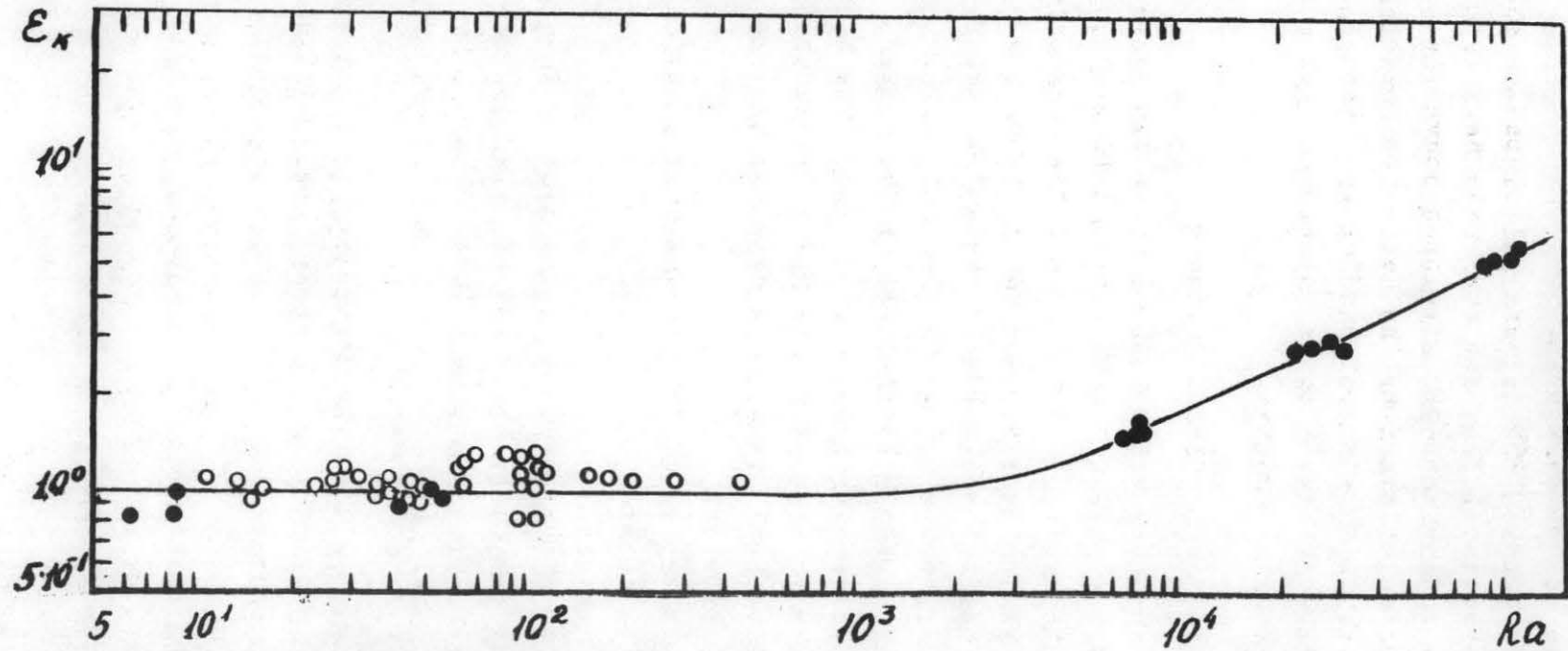


Fig.6. Dependence of coefficient  $E_k$  on the number  $Ra$

● - 19 rods

○ - 37 rods

been obtained at different pressure drops  $\Delta t'' \neq \Delta t'$  and at different average gap temperatures.

The values  $Q_{KONB}$  and  $Q_{KONG}$  were calculated as the difference between test heat flow and radiative heat flow.

In view of the analogy between developed convection in vertical and horizontal rod bundles the data from heat transfer tests in vertical and horizontal bundles were processed by the similar technique. Fig. 7 shows an average heat transfer curve for the vertical bundles.

#### Heat transfer in finned surfaces

Heat transfer analysis under natural convection have been carried out on the surfaces with vertical fins of height  $h = 100$  mm and depth  $S = 10$  mm. The fins and the base surface were constructed from carbonsteel (blackness degree  $E = 0,55$ ). The interfin spacing was  $S = 10, 15, 30, 40$  and  $80$  mm. The length of the working sections  $L = 285, 570$  and  $1010$  mm (Fig. 8). The sections were heated electrically by the heaters, mounted in the drilled holes of the base surface. The base and fin surfaces temperatures were measured by thermocouples and the average temperature in the gaps between fins was calculated.

The temperatures were used for average heat transfer coefficient calculation.

The test data shows:

- The decrease  $S$  from  $80$  mm to  $30$  mm at the section length  $L = 1010$  mm slightly changes the value of  $h$ , which remains significantly lower than the values, obtained for a single vertical plate. At  $S = 10$  mm the rate of heat transfer drops;
- When the section length decreases ( $L = 575$  and  $285$  mm) the change of  $S$  from  $40$  to  $15$  mm has a little effect on the heat transfer coefficients, which increases with  $L$  decrease, approaching the values for a single vertical plate. In processing average heat transfer data the interfin spacing  $S$  is used as a characteristic linear dimension, and the Reley number is multiplied by the ratio  $S/L$

$$R a_s^* = \frac{g\beta}{\nu\alpha} \cdot \Delta t \cdot S^3 \cdot \frac{S}{L}$$

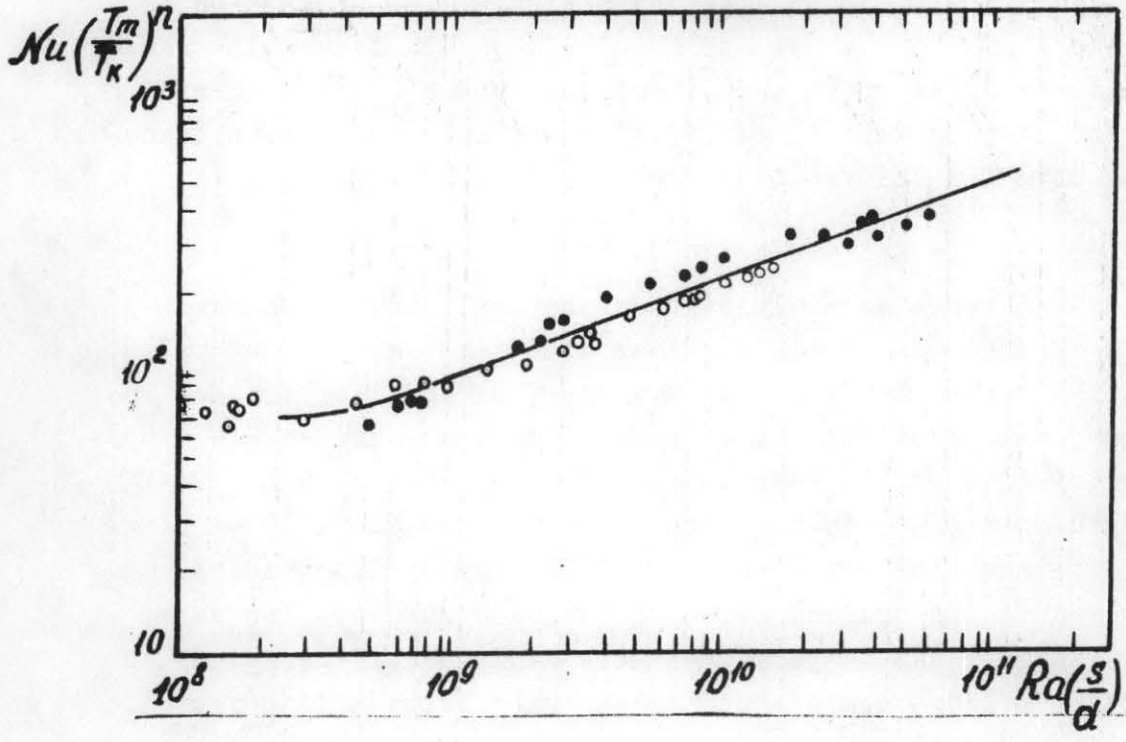


Fig.7. Function  $Nu (T_m / \bar{T}_k)^n = f (Ra \cdot s/d)$  for vertical rod bundles ( $\bar{t}$  - averaged)

- - 19 rods
- - 37 rods



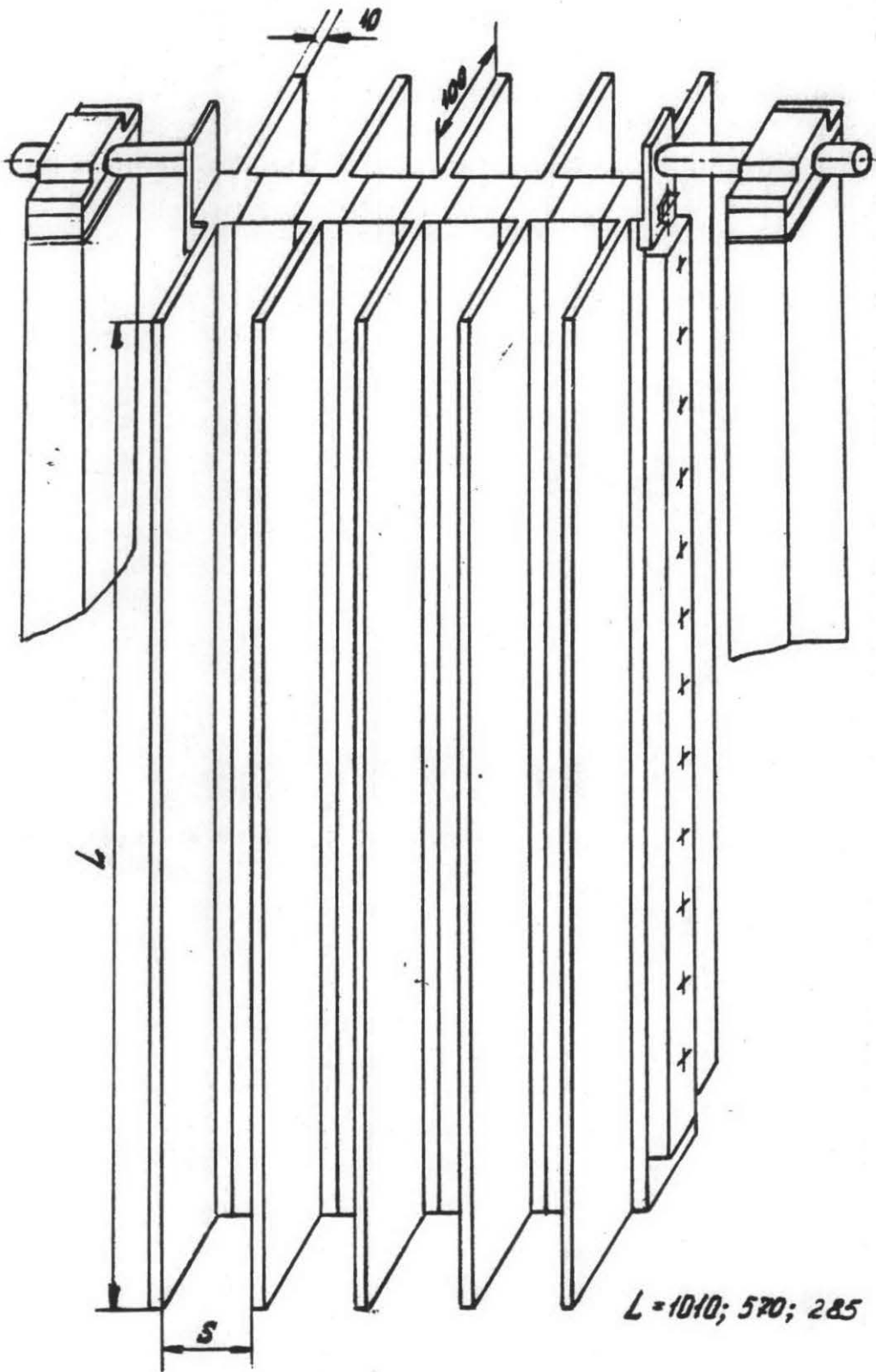


Fig.8. The experimental section.

Fig. 9 shows the curve for  $\overline{Nu}_s$  calculations. The similar curve for minimum heat transfer ( $Nu_s^{\min}$ ) calculation allows the base surface temperature to be determined.

The test data obtained from the section  $L = 0,570$  mm at different base slopes spaced  $\pi/4$  apart from horizontal to vertical position, allow horizontal package circular fins to be calculated with help of the above curves.

Computer code for a package thermal analysis under accidental fire conditions and subsequent cooling.

To determine the temperature patters in the shell, the cover and the neutron-shielding shell of a package the computer code was developed for two-dimensional solution of unsteady heat-transfer equations in an axially symmetric region.

The code algorithm is based on the synthesis of solutions for elementary circuled subregions approximating in the sum the original analysed region and forming the set of zones of intermediated division.

In each elementary subregion the equation in the following form is solved;

$$cp \frac{\partial T}{\partial z} = \kappa \frac{1}{r} \frac{\partial}{\partial r} \left( r \frac{\partial T}{\partial r} \right) + \kappa \frac{\partial^2 T}{\partial z^2} + \left( \frac{\partial T}{\partial z} + \frac{\partial T}{\partial r} \right) \left( \frac{\partial \kappa}{\partial r} + \frac{\partial \kappa}{\partial z} \right)$$

In the code described the following boundary conditions can be defined over the every side of any circular region (individually or in any reasonable combinations)

- continuous (contact)
- adiabatic
- convective heat flux proportional to the specified or calculated heat transfer coefficient and linear temperature difference
- the specified or calculated (variable) heat flux;
- the heat flux under radiative heat transfer in atmosphere or from radiative surfaces of variable temperature;
- heat transfer in gaps or in seals between package surfaces.

The temperature-dependent thermal properties of package materials are stored in a tabulated form and are retrieved by quadratic interpolation for every integration step.

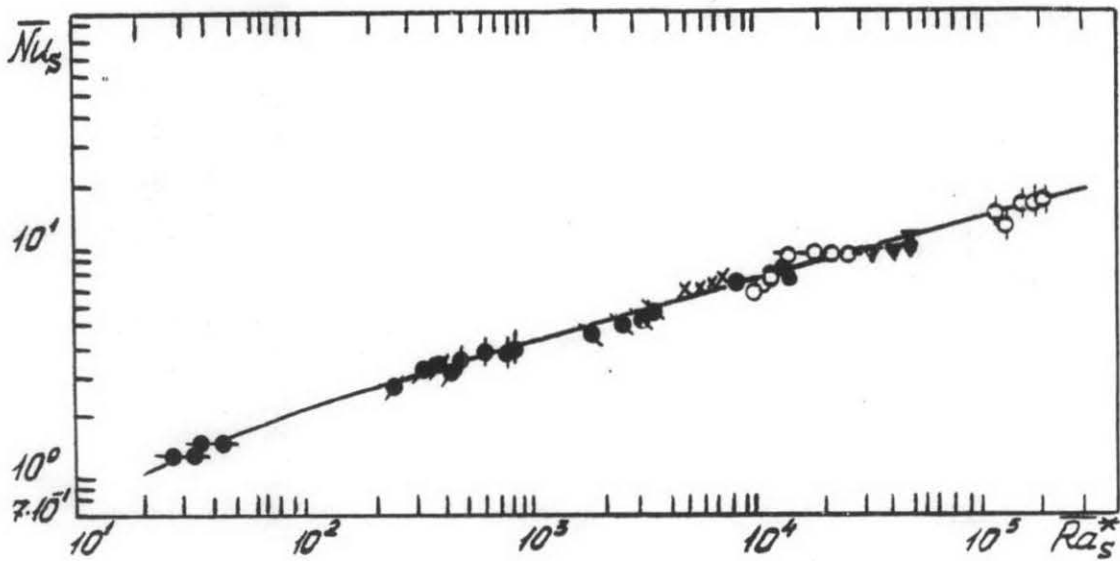


Fig.9. Average finned surface heat transfer under natural convection.

Test data.

L = 0,285 m

◊ - S = 15 mm

● - S = 30 mm

▼ - S = 40 mm

L = 0,57 m

■ - S = 15 mm

X - S = 30 mm

○ - S = 40 mm

L = 1,01 m

◐ - S = 10 mm

◑ - S = 30 mm

○ - S = 40 mm

◊ - S = 80 mm

The transition from the shell inner surface temperature to the maximum heated fuel element temperature in the maximum heated assembly proceeds with help of the thermal resistance, obtained on the basis of the package thermal analysis in steady state.

The analytical proof of package strength

The analytical proof of a package design compliance with requirements of "IAEA Regulations for the Safe Transport of Radioactive Materials" (IAEA-SM-147/8) has a number of advantages over the other techniques presented in the "IAEA Regulations". The most obvious advantage is the generalized results, obtained on the basis of the postulates of mechanics of deformable bodies or other laws of physics. The important advantages are the high speed of data processing, the possibility of trade off studies, low labour and money expenditures. Besides the analytical prediction is necessary for design of an experiment.

The peculiarity of the package strength analysis in comparison with that of the conventional heat transfer equipment is the fact, that the loads, applied at analysed components (a cover; cover fasteners, assemblies, a basket etc.) are not specified, but are determined by a package design. Thus, the general problem of a package strength analysis consists of two interrelated problems: the contact problem is to compute the dynamic loads, applied at the analysed design components, and the strength evaluation problem is to determine the reaction at the components to the dynamic loads.

The cover edge deformation depth calculation at 9-m drop on edge is the case of the contact problem. The rigid / elastic body deformation pattern is used and the deformation rate effect on yield strength is considered.

In such a way the expression for maximum edge deformation depth is obtained:

$$z_{\max} = 0,95 \cdot \kappa \cdot D^2 \left( \frac{T_0 \cdot L}{\sigma_r \cdot D^4} \right)^{2/5} \cdot \sqrt{L^2 + D^2}$$

where D - package diameter,

L - package length,

$\sigma_r$  - material yield strength,



$T_0$  - Kinetic energy of a package dropped,

$K$  - coefficient to account for deformation rate effect.

The maximum retarding force on the package impact against a rigid base is calculated by:

$$P_{\max} = 0.288 \cdot G_r \cdot \frac{L^{3/2} \cdot Z_{\max}^{3/2}}{D} \cdot (1 + D^2/L^2)^{5/4}$$

The calculated values agree well with test data.

The serviceability justification of hexahedral borated basket is the case of strength evaluation problem. It was not possible to test a full-scale package with a basket and assembly models. That is why the hexahedral basket tube with the assembly model have to be tested as a part of a package model, fabricated not to scale. In the drop from a certain height against a rigid base the hexahedral tube should be loaded with the impulses equal to the real ones.

To solve the problem the value and the form of impact loading impulse on real package have been preliminary calculated. Then the number and the geometry of model dumping fins have been analytically determined and a model drop height to simulate loading on real hexahedral basket tubes have been calculated.

Measured impact accelerations at tube supports and measured vibration accelerations in the middle of a span at the moment of a drop agreed in high degree (the error is less 10 %) with predicted data.

The relatively low cost of the model allows a set of tests to be carried out to prevent random errors and to increase the test reliability. To run a similar set of full-scale tests is a rather difficult problem.

The analytical approach is widely used in problems, concerned with package serviceability, for instance, among the problems is the proof of a package joint fasteners strength under conditions of drop on a cover edge, when the cover tends to open under inertial load. Accelerated material hardening is taken into account. In some cases the more intricate techniques of mechanics of deformable bodies have been used to consider elastic wave propagation and their interrelation with package components, for instance with an assembly of a package case and a cover.

The dynamic stability of flexible elements under shock compression is the special problem.

The developed computer codes are used for all the problems cited earlier. They give the possibility to prove package safety in accordance with all the requirements of "IAEA Regulations".

#### References

1. Vdevec N.V., Grivnin A.J., Gotovskij M.A., Pervickaja T.A., Fromzel V.N., Fedorovich E.D., Shleifer V.A., TVT, 24, 4 (1986), 716.
2. Gotovskij M.A., Grivnin A.J., Pervickaja T.A., Fedorovich E.D., Fromzel V.N., Shleifer V.A. In book: Heat-mass exchange-VG, Minsk, 12, (1984) 74.

# *Session IX-1*

---

---

**Package  
Testing**

---